The emerging clinical role of cardiovascular magnetic resonance imaging

Andreas Kumar MD MSc, David J Patton MD, Matthias G Friedrich MD FESC

A Kumar, DJ Patton, MG Friedrich. The emerging clinical role of cardiovascular magnetic resonance imaging. Can J Cardiol 2010;26(6):313-322.

Starting as a research method little more than a decade ago, cardiovascular magnetic resonance (CMR) imaging has rapidly evolved to become a powerful diagnostic tool used in routine clinical cardiology. The contrast in CMR images is generated from protons in different chemical environments and, therefore, enables high-resolution imaging and specific tissue characterization in vivo, without the use of potentially harmful ionizing radiation.

CMR imaging is used for the assessment of regional and global ventricular function, and to answer questions regarding anatomy. State-of-the-art CMR sequences allow for a wide range of tissue characterization approaches, including the identification and quantification of nonviable, edematous, inflamed, infiltrated or hypoperfused myocardium. These tissue changes are not only used to help identify the etiology of cardiomyopathies, but also allow for a better understanding of tissue pathology in vivo. CMR tissue characterization may also be used to stage a disease process; for example, elevated T2 signal is consistent with edema and helps differentiate acute from chronic myocardial injury, and the extent of myocardial fibrosis as imaged by contrast-enhanced CMR correlates with adverse patient outcome in ischemic and nonischemic cardiomyopathies.

The current role of CMR imaging in clinical cardiology is reviewed, including coronary artery disease, congenital heart disease, nonischemic cardiomyopathies and valvular disease.

Key Words: *Cardiovascular magnetic resonance; Clinical cardiology; Congenital heart disease; Diagnosis; Imaging*

Le rôle clinique émergent de l'imagerie cardiovasculaire par résonance magnétique

Utilisée comme mode de recherche il y a un peu plus de dix ans, l'imagerie cardiovasculaire par résonance magnétique (CRM) a rapidement évolué pour devenir un puissant outil diagnostique en cardiologie clinique régulière. Le contraste des images CRM est produit par les protons des divers environnements chimiques qui, par conséquent, procurent une imagerie à haute résolution et une caractérisation tissulaire spécifique *in vivo*, sans qu'il soit nécessaire d'utiliser le rayonnement ionisant au potentiel néfaste.

L'imagerie CRM permet d'évaluer la fonction ventriculaire régionale et globale et de répondre à des questions liées à l'anatomie. Les séquences CRM de pointe permettent toute une série d'approches de caractérisation tissulaire, y compris le dépistage et la quantification d'un myocarde non viable, œdémateux, enflammé, infiltré ou hyperperfusé. Ces changements tissulaires sont non seulement utilisés pour contribuer à repérer l'étiologie des myocardiopathies, mais permettent également de mieux comprendre la pathologie tissulaire *in vivo*. La caractérisation tissulaire CRM peut également permettre d'établir le stade du processus de la maladie. Par exemple, un signal T2 élevé est compatible avec un œdème et contribue à différencier une lésion myocardique aiguë d'une lésion chronique, et l'étendue de la fibrose myocardique perçue par IRM avec injection d'un agent de contraste est corrélée avec des issues négatives en cas de myocardiopathie ischémique ou non ischémique.

Le rôle actuel de l'imagerie CRM en cardiologie clinique est analysé, y compris la coronaropathie, la cardiopathie congénitale, les myocardiopathies non ischémiques et les affections valvulaires.

Starting as a basic research tool in cardiology as recently as 10 years ago, cardiovascular magnetic resonance (CMR) imaging has become a powerful diagnostic method and has entered the clinical arena.

In general, the strengths of the technique lie in its favourable safety profile and the ability to use specific image acquisition settings (sequences) to create a tissue-specific contrast. The signal obtained depends on the magnetic properties of protons in any tissue, which are determined by tissue composition. The range of contrast patterns can be extended by the use of contrast agents, which, for example, enables the identification of contrast-enhancing lesions. Currently available standard sequences offer a spatial resolution of as high as 1.0 mm × 1.0 mm in plane – substantially higher than that achieved by single photon emission computed tomography (SPECT) and positron emission tomography (PET) imaging. Temporal resolution is good, with the fastest sequences being able to acquire an image in approximately 15 ms to 30 ms.

A recent consensus statement of the leading international societies for cardiology and radiology (including the American College of Cardiology Foundation, the American College of Radiology and the Society for Cardiovascular Magnetic Resonance) recommended CMR imaging for a list of clinical indications (1), and the Canadian Cardiovascular Society together with leading imaging societies in Canada published a position statement summarizing the indications for CMR imaging in ischemic heart disease (2).

In the present review, we discuss the emerging role of CMR imaging in clinical cardiology.

CMR IN CONGENITAL HEART DISEASE

CMR is well suited for pre- and postoperative evaluation of congenital heart disease (CHD) because it offers advantages over other imaging modalities, including lack of ionizing radiation, which is particularly important because many CHD patients will require imaging studies in childhood or serial examinations throughout their lifetime; capacity for true three-dimensional (3D) imaging; accurate blood flow quantification; tissue characterization; and freely selectable imaging planes with wide fields of view that enable assessment of relationships between cardiac and vascular structures (3,4). Although echocardiography is the initial imaging modality for CHD in infants and children, CMR is of benefit in the presence of complex anatomy or in older patients whose echocardiographic views may be suboptimal (5,6). CMR has found an increasingly important role in the evaluation of morphology and pathophysiology of complex CHD at all ages, particularly in the assessment of great vessel anatomy, venous connections, extracardiac conduits and intracardiac baffles, and complex spatial

Stephenson CMR Centre at the Libin Cardiovascular Institute of Alberta, University of Calgary, Calgary, Alberta

Correspondence: Dr Matthias G Friedrich, Stephenson CMR Centre at the Libin Cardiovascular Institute of Alberta, University of Calgary, Foothills Medical Centre, Suite 0700-SSB, 1403-29th Street Northwest, Calgary, Alberta T2N 2T9. Telephone 403-944-8806, fax 403-944-8510, e-mail matthias.friedrich@ucalgary.ca

Received for publication April 3, 2008. Accepted October 11, 2008

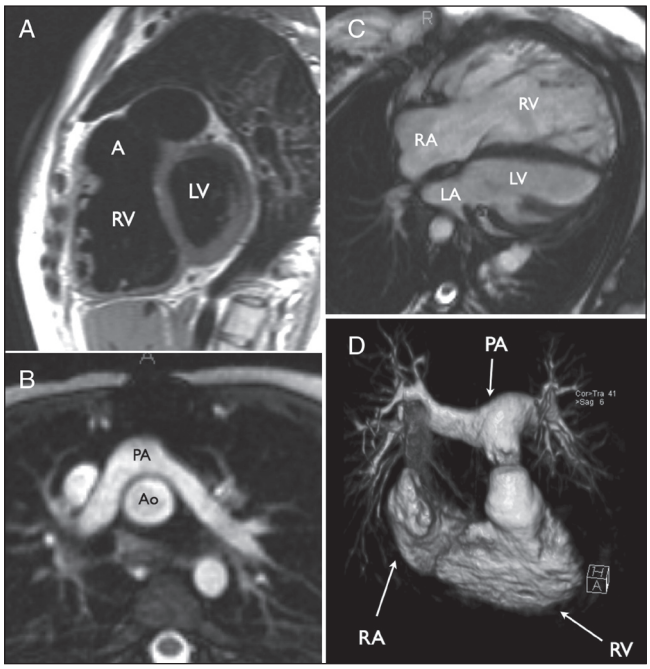

Figure 1) *Examples of cardiovascular magnetic resonance imaging of congenital heart disease.* **A** *Sagittal black-blood image of a patient with repaired tetralogy of Fallot, showing right ventricular dilation and an aneurysm (A) of the right ventricular outflow tract patch.* **B** *Transverse static bright-blood image (steady-state free precession) of the pulmonary arteries (PAs) lying anterior to the aorta (Ao) following arterial switch repair with the Lecompte manoeuvre in transposition of the great arteries.* **C** *Diastolic frame of a steady-state free precession cine image series in a patient with repaired tetralogy of Fallot and pulmonary regurgitation showing severe right ventricular dilation.* **D** *Volume rendering of a gadolinium-enhanced magnetic resonance angiogram of the right ventricle (RV) and PAs in a patient with an RV-to-PA-valved conduit for repair of pulmonary atresia and ventricular septal defect. LA Left atrium; LV Left ventricle; RA Right atrium*

relationships, as well as physiological evaluation of shunts, ventricular function and myocardial fibrosis (7).

The clinical use of CMR in patients with CHD – like that of any other imaging technique – is challenged by the tremendous diversity of congenital cardiac malformations and the manner in which they are repaired. Keeping in mind the versatility of CMR, the overall goals of CMR assessment of CHD include the following (8):

1. Evaluation of the anatomy and severity of the defect(s);
2. Assessment of the functional consequences of the defect(s) before and after surgical repair; and
3. Identification of associated and incidental lesions.

The first goal, anatomical evaluation, is achieved by imaging the heart and vascular structures in several planes to produce a multidimensional representation of the anatomy. Transverse, coronal, sagittal and oblique multislice images using black-blood sequences (fast spin echo) (Figure 1A) or static bright-blood sequences (static single-shot or segmented steady-state free precession [SSFP]) (Figure 1B) provide excellent anatomical definition and serve as reference images for accurate location of piloted breath-hold SSFP cine images, which are useful for assessment of anatomy and function. Contrast-enhanced magnetic resonance angiography with gadolinium, which has comparable diagnostic accuracy to x-ray angiography in complex CHD (9), is valuable for 3D assessment of extracardiac structures such as the aorta, main and branch pulmonary arteries, pulmonary veins and collateral vessels (Figure 1D). Time-resolved 3D contrast-enhanced magnetic resonance angiography is a newer angiographic technique that captures information about the dynamics of blood flow through the right and left heart using a small volume of contrast (10). Additionally, 3D static SSFP acquisitions may be obtained, either with single breath-hold or diaphragmatic monitoring, for visualization of the coronary arteries or 3D anatomy of the whole heart and vessels.

The second goal, assessment of the functional consequences of CHD, is achieved with a number of techniques including cine imaging using SSFP and phase-contrast velocity mapping. Cine imaging with SSFP offers an excellent contrast between blood and myocardium and, hence, is very useful for the analysis of right ventricular (RV) and left ventricular (LV) function (described in greater detail below), for quantification of ventricular volume and mass, and for the visualization of valve leaflets and high-velocity stenotic jets (Figure 1C). There are particular advantages of cine SSFP CMR imaging over echocardiographic evaluation of the right heart in CHD; CMR is independent of geometrical assumptions for evaluation of RV volume and function, and the wide field of view provides good visualization of the RV outflow tract and anterior RV wall. CMR quantification of the right ventricle is therefore becoming increasingly important in the management of patients with repaired tetralogy of Fallot and pulmonary regurgitation (11,12).

Evaluation of blood flow and velocity by CMR imaging is achieved with the use of phase-contrast velocity mapping, a technique that is based on magnetic resonant properties acquired from blood flowing in a magnetic field gradient. Phase-contrast maps acquired parallel to blood flow are used to measure peak velocities or assess turbulent jets. Phase-contrast velocity mapping allows measurement of blood flow as well as velocity. In this regard, phase-contrast techniques are useful for evaluation of flow, stenosis and regurgitation in the systemic and pulmonary circulations (13,14), and in shunt quantification in CHD (15).

The third goal, identification of associated and incidental lesions, relates to the complexity of many types of CHD. Because CMR produces images independent of acoustic windows and provides additional information about tissue characteristics such as myocardial scarring or fibrosis (described in greater detail in following sections of the present review), it may provide additional new diagnoses or insight into the pathophysiology of a patient's condition. For example, CMR is valuable in the detection of previously unrecognized shunts, aberrant arterial vessels (16) or anomalous pulmonary veins (17). Additionally, CMR findings of myocardial fibrosis or infarction in repaired transposition of the great arteries (18) and in tetralogy of Fallot (19) appear to have prognostic significance with respect to ventricular function, exercise tolerance, arrhythmia or sudden death in these types of CHD.

CMR FOR THE ASSESSMENT OF RV AND LV SIZE AND FUNCTION

CMR provides accurate measurements of LV and RV mass, volumes and systolic function. SSFP sequences are commonly used and provide excellent contrast of myocardium over intracavitary blood, and cine movies covering one cardiac cycle with 25 frames are typically acquired over 15 heartbeats (with acquisition of up to six slices during one breath-hold) (20). Using the multiple short-axis slice-summation method, contiguous slices of short-axis cine datasets are acquired from the base of the left ventricle to the apex, covering the myocardium completely. This approach has been shown to provide excellent accuracy (21) and low interstudy variability (22); normal values are available for healthy subjects (23). A less commonly used approach covers the entire LV myocardium with multiple radial long-axis slices, and has been shown to yield similarly robust values of interobserver variability (24). Imaging time for the acquisition of a complete LV or RV data set takes in the range of 3 min to 5 min, and approximately 5 min to 10 min are required for quantitative data analysis. In the absence of arrhythmia, CMR yields a consistently stable image quality, and the reproducibility of CMR for anatomical and functional parameters is higher than that of echocardiography (25). This translates into a sample size reduction in research studies when CMR is used to measure

treatment effects on ventricular volumes, function or mass (26-28), and it allows higher accuracy in the assessment of smaller changes of these parameters in patients. Furthermore, two-dimensional (2D) echocardiographic studies have been shown to overestimate LV mass and underestimate LV volume when compared with CMR imaging (29). This is explained by the technical approach to volumetric assessment. While 2D echocardiography obtains quantitative data in two imaging planes, these are subsequently extrapolated to obtain 3D data, under the assumption that the patient's ventricle has a geometrical ellipsoid shape. This, however, may not perfectly represent the patient's anatomy. CMR overcomes this limitation by using a 3D imaging method; here, volumes are measured, not extrapolated, and anatomical variances are respected. In summary, while 2D echocardiography can provide an estimate of LV volumes and function, CMR can provide an actual measurement of LV volumes and function; therefore, it is often regarded as the gold standard for the assessment of ventricular volumes and function.

Few approaches have been undertaken to examine diastolic dysfunction with CMR, but none is currently being widely used in routine clinical imaging. One promising approach uses a technique known as tagging. Here, magnetic field saturation is applied to the myocardium in a grid-like fashion, and the deformation of this grid is used to assess regional wall motion and strain (30,31). However, analysis software is currently too complex for daily routine use. One working group has suggested tissue phase mapping of the myocardium as an alternative for diastolic function assessment. This method measures myocardial tissue velocity in 3D space, which can be used to measure diastolic wall motion with low interobserver variability (32).

DETECTION OF STRESS-INDUCED MYOCARDIAL ISCHEMIA

CMR currently offers two clinically used methods for the detection of stress-induced myocardial ischemia – first-pass perfusion studies with a vasodilatory stress agent (adenosine) (Figure 2), and wall motion analysis with an adrenergic agent (usually dobutamine). Both are routinely used in experienced CMR centres, with modern cardiac scanners allowing for continuous real-time electrocardiographic and respiratory monitoring, blood-pressure measurements and intercom systems for optimal patient supervision.

Adenosine causes microvascular vasodilation by acting on the A2 receptors of the muscularis layer of coronary resistance vessels. Although adenosine is used to unmask hypoperfused myocardium at perfusion scans, the underlying mechanism of action is not well understood. It is commonly believed that adenosine causes a 'steal phenomenon' by increasing perfusion in coronary territories not affected by epicardial artery stenosis, which leads to relative hypoperfusion of the territory subtended by a stenosed coronary artery (33). Several research papers (34-38), including one multicentre study, have assessed the role of adenosine stress perfusion for the diagnosis of coronary artery disease and consistently demonstrated high sensitivity for CMR imaging to diagnose epicardial coronary artery stenoses. When CMR perfusion was compared with x-ray coronary angiography, its specificities to detect coronary stenoses were only moderately high (62% to 90%) (34-38). However, when PET or fractional flow reserve on x-ray angiography were used as standards of truth, specificities were higher (94% [34] and 90% [38], respectively). This is explained by the fact that CMR assesses perfusion on a tissue level, which includes not only perfusion deficits caused by macrovascular epicardial coronary artery disease, but also those due to microvascular disease as it occurs, for example, in diabetes or chronic arterial hypertension. The method can be used to quantify myocardial perfusion reserve with good interobserver and intraobserver variabilities (36). In patients presenting to the emergency room with chest pain and exclusion of acute myocardial infarction, abnormal findings on adenosine stress perfusion were shown to predict adverse cardiovascular events independently and stronger than the combination of known risk factors; furthermore, negative adenosine stress perfusion tests had a negative predictive

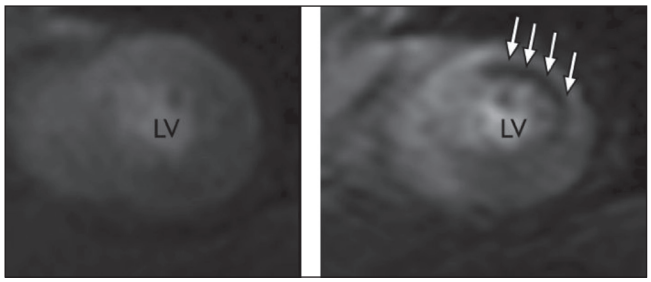

Figure 2) *Adenosine stress perfusion imaging of a patient with coronary artery disease. A patient with a high-grade stenosis of a diagonal branch artery. The left image shows a short-axis view of an apical short-axis slice (still frame extracted from a movie). There is no significant perfusion deficit during contrast infusion at rest. When the examination is repeated 20 min later during the continuous infusion of adenosine, the second contrast infusion shows a stress-induced subendocardial perfusion deficit of the anterolateral wall (arrows). LV Left ventricle*

value of 100% for cardiovascular events at one-year follow-up in one study (39). A high negative predictive value was recently confirmed in another study involving more than 450 stable outpatients who were referred for a CMR stress test (40).

Dobutamine stress studies for ischemia-induced wall motion abnormalities can be performed with CMR protocols identical to those established for transthoracic dobutamine stress echocardiography, with a similar safety profile (41-43). Because wall motion abnormalities occur later in the ischemic cascade than perfusion deficits (44), dobutamine stress tests may be less sensitive but more specific for inducible ischemia than perfusion tests.

An advantage of CMR imaging over transthoracic echocardiography for dobutamine stress testing is that state-of-the-art CMR sequences offer consistently high image quality for visualization of all RV and LV wall segments. Additionally, CMR is not limited by the restrictions of an acoustic window. In a head-to-head comparison of more than 200 patients, this was shown to translate into superior accuracy of dobutamine stress CMR imaging (accuracy 86%) over echocardiography (accuracy 73%) for the diagnosis of epicardial coronary artery disease (45). Overall, published sensitivities for the diagnosis of epicardial coronary artery stenosis using dobutamine stress CMR imaging are reported to be in the range of 78% to 89%, with specificities in the range of 80% to 87% (45-47).

Few working groups have studied blood oxygen level-dependent CMR imaging as a method to detect adenosine-dependent ischemia in coronary artery disease. This approach does not depend on a contrast agent, and derives image contrast from the concentrations of oxygenated versus deoxygenated hemoglobin. While early studies (48,49) demonstrated the feasibility of this approach, they were limited by image artifacts; recent technical developments have overcome this problem, and more recent research (50,51) suggests that blood oxygen level-dependent CMR imaging may be entering the clinical arena in the next few years as a test for myocardial hypoxemia.

ASSESSMENT OF MYOCARDIAL VIABILITY IN ISCHEMIC HEART DISEASE

The detection of viable myocardium plays a crucial role in clinical cardiology because it has been shown that myocardial infarction patients only benefit from revascularization therapy if the reperfused tissue is viable (52,53).

In a clinical setting, there are two ways to assess myocardial viability with CMR – cine imaging, which allows for wall motion analysis at rest and during low-dose dobutamine stress; and 'late enhancement' imaging, which identifies nonviable tissue (fibrosis and scar).

Low-dose dobutamine stress CMR imaging for viability assessment is performed with protocols similar to low-dose dobutamine stress echocardiography. An improvement of regional contractility

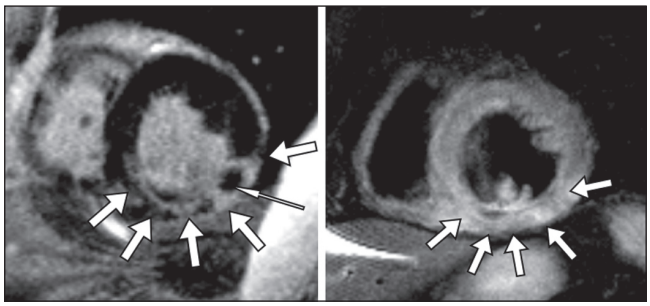

Figure 3) *A patient with an acute posterolateral myocardial infarction. The image to the left displays a short-axis view using the 'late enhancement' sequence after application of gadolinium-diethylene triamine penta-acetic acid contrast. There is contrast enhancement indicating myocardial necrosis of the inferior lateral wall (bold arrows), but not in the anterior and septal wall. There is an area of microvascular obstruction, highlighted with the slim arrow. The image to the right is a T2-weighted spin-echo image, showing a regionally high signal in the inferior lateral wall (arrows), consistent with myocardial edema in the area of necrosis. The presence of edema indicates that the infarction is acute*

during a continuous infusion of dobutamine at a dose of 10 µg/kg body weight/min or less has been shown to be a powerful predictor of functional recovery after revascularization therapy (54), and is a better predictor of LV functional recovery after revascularization than end-diastolic wall thickness (55). However, this method is limited by assessing viability indirectly through an assessment of function as a surrogate, which can be hampered in the presence of dysfunctional (eg, stunned or hibernating) tissue (56).

A more recently developed approach allows for viability assessment at the tissue level and is known as 'late enhancement' imaging. The method, first described by Simonetti et al (57) and first used by Kim et al (58), is based on gadolinium contrast enhancement of nonviable cardiac tissue (Figure 3); it accurately reflects infarction tissue when compared with ex vivo pathology in animal models (57-60) and is highly reproducible (61). The underlying mechanism is an increased volume of distribution for the extracellular contrast agent gadolinium-diethylene triamine penta-acetic acid in nonviable tissue as opposed to healthy myocardium, leading to delayed washout of contrast in nonviable tissue (60,62). In addition to contrast enhancement of myocardial necrosis or collagenous scar, late enhancement imaging sequences suppress the signal derived from remote noninfarcted myocardium, leading to very high image contrast. Image voxel size obtained with these sequences is typically 1.5 $mm^2 \times 1.3$ mm^2 in plane with a slice thickness of 8 mm or 10 mm, which allows the detection of myocardial infarcts involving as little as 0.7 g of tissue (63). The method is established in acute as well as chronic myocardial infarction.

The high spatial resolution viability imaging allows for the in vivo assessment of the transmural extent of viable myocardium as well as the amount of viable tissue within one segment of myocardium. The spatial resolution is superior to what is achieved by SPECT or PET imaging and, consequently, subendocardial infarctions that are missed by SPECT (59,64,65) and PET imaging (66,67) are detected by late enhancement CMR imaging.

The transmural extent of late enhancement contains clinically relevant information because it can be used to predict the functional recovery of myocardial contractility after vascularization. In a study performed by Choi et al (68) in patients with acute reperfused myocardial infarction, only 5% of segments demonstrated improved contractility at eight to 12 weeks follow-up if the transmural extent of necrosis was greater than 75%; however, it was 63% when the transmural extent of necrosis was 50% or less. Other investigators confirmed the correlation of functional recovery with transmural extent of viable tissue in acute myocardial infarction (69) as well as in chronic ischemic disease (70,71). Equally, in chronic systolic heart failure, the recovery of function after initiation of beta-blocker therapy was shown to be a measure of the transmural extent of viable myocardium (72). CMR imaging is therefore a useful tool to assess stunned as well as hibernating (73) myocardium, when functional cine imaging is combined with late enhancement imaging. CMR imaging has a higher accuracy than SPECT for the prediction of functional recovery, which is explained by the higher spatial resolution of CMR (65).

More recently, the concept of peri-infarct zone imaging was introduced using CMR imaging. Electrophysiology studies have suggested that in ischemic heart disease, the infarct border zone may be the origin of ventricular tachycardia due to micro re-entry. Initial CMR studies have shown an association between the extent of the heterogeneous infarct border zone and inducible ventricular tachycardia (74) and mortality, independent of ejection fraction, infarct size and ventricular volume (75).

The same technique applied early after contrast injection is used for visualization of microvascular obstruction or no reflow, which presents as absence of contrast enhancement in the subendocardium, surrounded by contrast enhancement in the infarcted but successfully reperfused tissue (Figure 3). The presence of no reflow, as displayed on CMR imaging, predicts adverse outcome independent of infarct size (76).

While late enhancement CMR imaging is highly accurate for the detection of viable myocardium, it is unable to differentiate between acute necrosis and chronic fibrotic scar.

Advancement in CMR imaging was achieved when T2-weighted spin-echo imaging was shown to yield a signal increase specific to acute, but not chronic, myocardial infarction (77). The signal intensity in T2-weighted images is influenced by the tissue water content, and myocardial edema is believed to be the main underlying pathology that causes the T2 signal change. Myocardial edema precedes myocardial necrosis (78), and is a marker of the area at risk in acute ischemia (79,80). T2 signal changes persist after reperfusion, and this method can therefore be used to determine the area at risk retrospectively after reperfusion therapy. In conjunction with infarct size measurement, the myocardial salvage can be measured in grams of tissue (77,79-81). A recent study (82) suggested that edema in reversibly injured myocardium may be the cause of myocardial stunning in acute ischemic injury.

In summary, the combination of functional studies, sequences for stress-inducible ischemia, viability and edema allow for the comprehensive assessment of a patient with coronary artery disease within 30 min to 40 min of examination time. Example images of a viability study in a patient with acute myocardial infarction are shown in Figure 3.

CMR FOR PATIENT ASSESSMENT BEFORE CARDIAC RESYNCHRONIZATION THERAPY

Two types of CMR parameters have been assessed for patient evaluation before cardiac resynchronization therapy (CRT) – functional parameters that assess different aspects of ventricular wall motion, and tissue characterization parameters that assess myocardial scar. In terms of functional LV assessment, velocity-encoded CMR of LV contraction has been shown to yield similar results as tissue Doppler echocardiography (83). Moreover, CMR tagging allows for the assessment of regional function, which can be used to assess circumferential shortening and regional quantification of myocardial strain. A recent study suggested that strain imaging may be more effective at predicting response to CRT than the assessment of mechanical dyssynchrony (84); however, another study demonstrated that a CMR function-derived dyssynchrony index is of prognostic value and useful for the prediction of mortality and morbidity after CRT (85).

The second way to predict response to CRT using CMR imaging is the assessment of scar burden using late enhancement CMR imaging. Several studies have demonstrated that an increased scar burden, measured as total scar or transmural extent of scar, decreases the likelihood of a patient to respond to CRT. The relationship between scar burden and LV end-systolic volume at six months post-CRT appears to be linear (86), but scar location in the septum (87) or transmural extent of the scar (88) may be more powerful predictors of response than global scar burden.

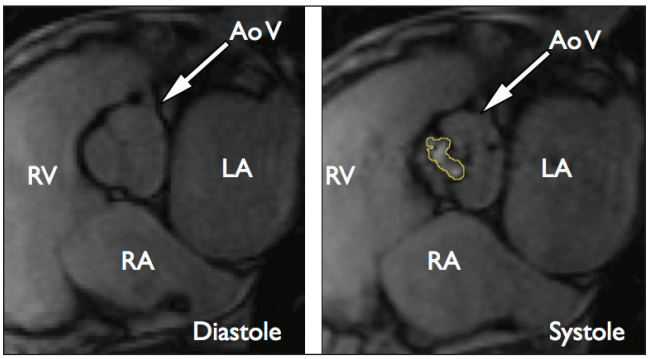

Figure 4) *A patient with aortic valve stenosis. Both images are still frames extracted from steady-state free precession cine movies. The orifice of the aortic valve can be measured from the systolic image to the right. The contour of the orifice is marked in yellow. AoV Aortic valve; LA Left atrium; RA Right atrium; RV Right ventricle*

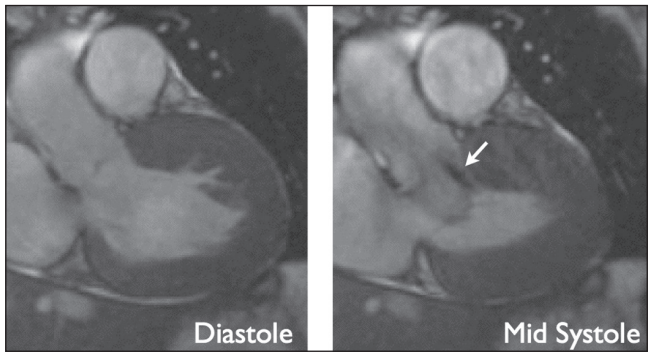

Figure 5) *A patient with hypertrophic obstructive cardiomyopathy. Both images are extracted from functional steady-state free precession cine movies, at diastole (left) and mid-systole (right). The diastolic image displays marked thickening of the anterior septal wall. At mid-systole, there is an anterior movement of the anterior mitral valve leaflet, causing left ventricular outflow tract obstruction and a jet of high-velocity flow (arrow). Cardiovascular magnetic resonance imaging allows for quantification of the obstruction by planimetry of the left ventricular outflow tract and flow velocity quantification of the jet (not shown)*

While these approaches yield very promising initial data, the best possible way to assess CRT response and to predict mortality after this procedure using CMR is still a matter of ongoing research.

VALVULAR HEART DISEASE

CMR can quantify the severity of regurgitant and stenotic valvular lesions. Several methods are available for this purpose – phase-contrast sequences quantify anterograde and retrograde flow volumes and velocities in any desired imaging plane, within a vessel or a valvular plane (89,90). The accuracy of phase-contrast measurements as assessed with in vitro models is excellent (91,92) and good correlations have been documented between CMR flow measurements and Doppler echocardiography (93), as well as cardiac catheterization (94,95). Cine imaging is applied to quantify the orifice of a stenotic valve (96).

Aortic valve stenosis can be accurately quantified by planimetry of the aortic valve (96,97) (Figure 4), a method that does not depend on pressure gradient measurement-derived calculations, and that therefore may be less susceptible to pre- and afterload variations. Another established way to assess the aortic valve area is by flow measurements using phase-contrast CMR imaging, analogous to Doppler echocardiography. This CMR method allows calculation of the pressure gradient and valve area, but does not directly measure the orifice; it shows good correlation with the values obtained by Doppler echocardiography (93). Aortic regurgitation can be measured by characterization of blood flow immediately adjacent to the aortic valve, using phase-contrast magnetic resonance imaging. This allows for the calculation of regurgitant volume and regurgitant fraction. The method is highly reproducible (98), and the results agree well with aortic root angiography (94). Similar principles are applied to the assessment of the mitral and right-sided heart valves (95,99,100).

CMR IMAGING OF NONISCHEMIC CARDIOMYOPATHIES

CMR imaging can principally make two contributions to the workup of patients with nonischemic cardiomyopathies:

1. Identification of the etiology of the nonischemic cardiomyopathy; and
2. Quantification of volume, mass and systolic function of the right and left ventricles, and quantification of scar tissue as measures of disease severity.

Identification of etiology

Hypertrophic cardiomyopathy: In hypertrophic cardiomyopathy, CMR can identify the pattern of hypertrophy (eg, differentiation between global and regional hypertrophy, with or without LV outflow tract obstruction) using the aforementioned sequences for ventricular function. The accuracy of the method for quantification of LV mass and systolic function makes it an appropriate tool for the serial follow-up of a patient with sensitive evaluation of the effects of pharmacological therapy. LV outflow tract obstruction can be identified (101) and quantified before and after therapeutic septal artery embolization; the change in outflow tract dimensions was shown to correlate with the improvement of the patient's symptoms (Figure 5) (102). On histology, the disease is known to cause myofibrillar disarray and fibroses at the insertion sites of the RV wall; this is reflected by a signal increase on late enhancement imaging in those regions (103-105). Some studies (104) suggested that an increasing amount of fibrotic areas correlates with increasing clinical predictors for sudden cardiac death in patients with hypertrophic cardiomyopathy. A large prospective study (106) demonstrated an association between the extent of late enhancement and the occurrence of ventricular arrhythmia. Late enhancement may, therefore, emerge as a prognostic tissue marker in hypertrophic cardiomyopathy. However, more prospective mortality data are needed.

Idiopathic dilated cardiomyopathy: Idiopathic dilated cardiomyopathy is characterized by an increase in end-diastolic volume and, usually, reduced systolic function of the left and right ventricles; histopathology reveals partial replacement of cardiomyocytes by fibrotic tissue. LV dilation is readily identified by CMR using 3D assessment of ventricular volumes and systolic function. Further insight can be obtained by adding tissue characterization sequences to the CMR examination. Idiopathic dilated cardiomyopathy does not display any late enhancement in two-thirds of patients, but in one-third of patients, focal fibrosis of the septum is observed at the mid-wall level, commonly termed the 'mid-wall sign' (107,108). The presence of this finding was recently identified as a prognosticator of adverse outcome, and it is also a substrate of ventricular tachycardia (108,109).

A diagnostic challenge that cardiologists face frequently is the need for differentiation of idiopathic dilated cardiomyopathy from phenotypic dilated cardiomyopathy as a secondary result of an unidentified primary disease. The phenotype of dilated cardiomyopathy is frequently caused by ischemic cardiomyopathy, but among many others, may be caused by myocarditis (110), exposure to cardiotoxic agents such as drugs (eg, anthracyclines) (111), alcohol abuse (112) and autoimmune diseases (113).

CMR tissue characterization can play a crucial role in this situation, because the pattern of fibrosis seen on late enhancement CMR imaging allows differential diagnosis of the underlying disease. In

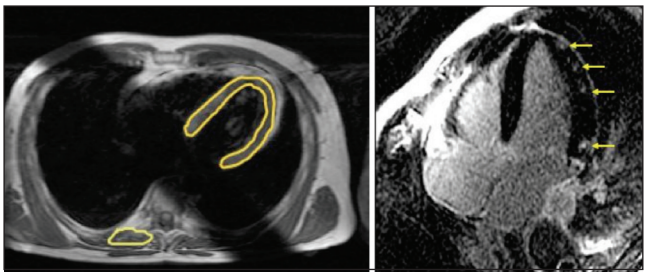

Figure 6) *A patient with myocarditis. The quantitative measurements of signal intensities in the myocardium normalized to skeletal muscle using a T1-weighted spin-echo sequence, before and after application of gadolinium contrast, allow for identification of patients with inflammatory myocardial disease (left image). In patients with acute severe myocarditis, patchy foci of delayed enhancement can be visualized, corresponding to foci of acute myocardial necrosis (right image, arrows)*

ischemic cardiomyopathy, CMR imaging displays infarction-type scar tissue usually restricted to the perfusion territory of one coronary artery, extending across the myocardium from the subendocardium. In anthracycline toxicity, late enhancement has been observed in a global subendocardial fashion (114), and early enhancement (a measure of hyperemia and capillary leak) is increased (115). Myocarditis is diagnosed using a comprehensive tissue assessment.

Myocarditis

Myocarditis leads to inflammatory tissue changes including hyperemia, capillary leak, edema and, in severe cases, cardiomyocyte necrosis that remodels to fibrosis.

For the diagnosis of inflammatory tissue changes in myocarditis, several CMR sequences are available that specifically address these different aspects of tissue pathology:

- T1-weighted early contrast-enhanced sequences assess myocardial hyperemia and capillary leak (116);
- T2-weighted sequences assess myocardial edema (117,118); and
- Late enhancement assesses cardiomyocyte necrosis or fibrosis (119,120).

Therefore, a comprehensive in vivo assessment of tissue pathology is possible, beyond the analysis of myocardial volumes and function.

The fibrosis and edema patterns observed in myocarditis are often patchy and, unlike in myocardial infarction, do not necessarily involve subendocardial areas (Figure 6) (117). Some studies observed that the epicardium of the inferior lateral wall was affected more often than other areas (119); other studies linked certain fibrosis patterns to specific causative viruses (120). It was shown that early enhancement changes are detectable soon after the clinical onset of disease and vanish with declining symptoms at follow-up (121). Two studies from independent working groups have shown that sequences that assess edema and hyperemia are more sensitive, while late enhancement imaging is more specific for the diagnosis of myocarditis (117,118). This is in accordance with the current understanding of pathophysiology. While inflammatory changes with edema and hyperemia are a mandatory component of inflammation in myocarditis, tissue necrosis may only occur in more severe cases. Both studies showed that the highest diagnostic accuracy is achieved by combining different tissue characterization methods in one diagnostic study and, therefore, assessing several aspects of tissue pathology at the same time. In a recent expert consensus conference on the CMR diagnosis of myocarditis, a combination of functional imaging, T2-weighted imaging, and early and late enhancement was recommended as the approach of choice for patients with suspected myocarditis (122). This combined approach yielded a sensitivity of 76%, a specificity of 95.5% and an accuracy of 85% for the diagnosis of acute myocarditis in a study applying comprehensive clinical information as a reference standard (117). Another study of patients with chronic active myocarditis, using myocardial biopsy with histology and immunohistology as a reference standard, yielded a sensitivity of 62%, a specificity of 89% and a diagnostic accuracy of 74% (118). In a recent review paper (123), CMR imaging was considered to be the most powerful noninvasive tool for determining whether active myocarditis is present.

Other nonischemic cardiomyopathies

The principle of using different imaging sequences to enable tissue characterization of the myocardium is also useful in other cardiomyopathies. CMR imaging detects myocardial involvement in amyloidosis; late enhancement involves the myocardium globally, usually with a predominant involvement of the subendocardium (124,125). Cardiac involvement in sarcoidosis can be diagnosed by early and late contrast enhancement. Early enhancement reflecting hyperemia is a more sensitive method (126), and late enhancement may identify patients with a worse clinical course. The late enhancement pattern involves the lateral wall more frequently than other areas of the myocardium (126-128).

Myocardial involvement in Anderson-Fabry disease leads to myocardial fibrosis, which can be visualized by late enhancement CMR imaging (129,130). The amount of fibrotic tissue as defined by late enhancement imaging correlates well with the extent of LV hypertrophy, and it is more frequently observed in the inferior lateral wall. The subendocardium is usually spared, which helps to differentiate this disease from others.

In thalassemia, progressive iron deposition in the myocardium can lead to heart failure. Dedicated T2-star (T2*)-weighted CMR sequences can create image contrast depending on the iron content of the myocardium (131). These are used to detect cardiac involvement in thalassemia, and furthermore measure the T2* magnetic resonance value to quantify the amount of iron deposits in the myocardium. The amount of iron as assessed by in vivo T2* quantification correlates with LV systolic function (131). CMR imaging can be used to guide therapy in these patients, and a therapy-related reduction in iron content, as measured by CMR imaging, correlates with improvement in LV systolic function (132,133)

Noncompaction cardiomyopathy is caused by genetic abnormalities of the desmoglein gene and leads to a phenotype with regional LV wall thinning of the compact myocardium and increased trabeculation in the same area. However, a similar phenotype may also evolve as the result of remodelling in other cardiomyopathies. A CMR study comparing noncompaction cardiomyopathy to hypertrophic cardiomyopathy, aortic valve stenosis, dilated cardiomyopathy and hypertensive cardiomyopathy showed that CMR imaging is able to diagnose noncompaction with 86% sensitivity and has 99% specificity to differentiate it from other causes of hypertrabeculation, using simple diagnostic criteria (134). The increased trabeculation may be subject to fibrosis or hypoperfusion (135).

Few studies (136) have been published using CMR imaging in patients with transient LV apical ballooning (takotsubo cardiomyopathy). One case study (137) demonstrated edema and hyperemia in a patient with a typical takotsubo-like presentation. Late enhancement may also be present (138), indicating that cardiomyocyte necrosis can occur.

FURTHER CLINICAL APPLICATIONS OF CMR

In clinical practice, CMR is of important value for the diagnosis of aortic diseases. 3D contrast angiography is an excellent tool for the assessment of aortic aneurysms, and has high sensitivities and specificities for the diagnosis of aortic dissection (139). The combined use of different sequences providing T1 and T2 contrast, with and without fat suppression, perfusion imaging and assessment of contrast uptake, allow for noninvasive tissue characterization of cardiac and paracardiac masses (140). Additionally, high-resolution images can be obtained to exactly assess the spatial extent of a tumour.

Considerable effort is being invested in the development of CMR coronary angiography. Although the diagnostic accuracy appears to be comparable with computed tomography (141), the technique is not widely accepted as a routine clinical tool. Most studies agree on a limited image quality for middle and distal segments of the large epicardial

vessels, while image quality in the proximal segments is usually good (142).

SUMMARY AND CONCLUSION

Starting as a research tool little more than a decade ago, CMR imaging has entered the arena of routine clinical imaging applications. Specific imaging sequences and protocols are now available for a wide range of heart diseases, including ischemic and nonischemic heart disease, as well as valvular disease. The high accuracy of flow measurements, freedom to deliberately choose an imaging plane and the lack of ionizing radiation make it the imaging modality of choice for CHD in children and adults. The unique ability to obtain information on disease-specific tissue characteristics provides the clinician with new insight into pathology and pathophysiology in vivo. Although long-term follow-up studies with very large patient numbers remain scarce, there is evolving evidence that some pathological CMR imaging findings, such as fibrosis, may be of value as predictors of patient outcome.

DISCLOSURE: Andreas Kumar MD prepared this manuscript as a Canadian Institutes of Health Research strategic training fellow in the Tomorrow's Research in Cardiovascular Health Professionals (TORCH) Program. The authors thank Dr Jordin D Green for critical revision of this manuscript.

REFERENCES

1. Hendel RC, Patel MR, Kramer CM, et al. ACCF/ACR/SCCT/SCMR/ASNC/NASCI/SCAI/SIR 2006 appropriateness criteria for cardiac computed tomography and cardiac magnetic resonance imaging: A report of the American College of Cardiology Foundation Quality Strategic Directions Committee Appropriateness Criteria Working Group, American College of Radiology, Society of Cardiovascular Computed Tomography, Society for Cardiovascular Magnetic Resonance, American Society of Nuclear Cardiology, North American Society for Cardiac Imaging, Society for Cardiovascular Angiography and Interventions, and Society of Interventional Radiology. J Am Coll Cardiol 2006;48:1475-97.
2. Beanlands RS, Chow BJ, Dick A, et al. CCS/CAR/CANM/CNCS/CanSCMR joint position statement on advanced noninvasive cardiac imaging using positron emission tomography, magnetic resonance imaging and multidetector computed tomographic angiography in the diagnosis and evaluation of ischemic heart disease – executive summary. Can J Cardiol 2007;23:107-19.
3. Simonetti OP, Cook S. Technical aspects of pediatric CMR. J Cardiovasc Magn Reson 2006;8:581-93.
4. Valente AM, Powell AJ. Clinical applications of cardiovascular magnetic resonance in congenital heart disease. Cardiol Clin 2007;25:97-110,vi.
5. Marcu CB, Beek AM, van Rossum AC. Clinical applications of cardiovascular magnetic resonance imaging. CMAJ 2006;175:911-7.
6. Pennell DJ, Sechtem UP, Higgins CB, et al. Clinical indications for cardiovascular magnetic resonance (CMR): Consensus Panel report. Eur Heart J 2004;25:1940-65.
7. Fogel M. CMR in congenital heart disease. In: Lardo A, Fayed ZA, Chronos NAF, Fuster V, eds. Cardiovascular Magnetic Resonance: Established and Emerging Applications. New York: Martin Dunitz, 2003:201-30.
8. Wood JC. Anatomical assessment of congenital heart disease. J Cardiovasc Magn Reson 2006;8:595-606.
9. Geva T, Greil GF, Marshall AC, Landzberg M, Powell AJ. Gadolinium-enhanced 3-dimensional magnetic resonance angiography of pulmonary blood supply in patients with complex pulmonary stenosis or atresia: Comparison with x-ray angiography. Circulation 2002;106:473-8.
10. Finn JP, Baskaran V, Carr JC, et al. Thorax: Low-dose contrast-enhanced three-dimensional MR angiography with subsecond temporal resolution – initial results. Radiology 2002;224:896-904.
11. Dave HH, Buechel ER, Dodge-Khatami A, et al. Early insertion of a pulmonary valve for chronic regurgitation helps restoration of ventricular dimensions. Ann Thorac Surg 2005;80:1615-20; discussion 1620-1.
12. Therrien J, Provost Y, Merchant N, Williams W, Colman J, Webb G. Optimal timing for pulmonary valve replacement in adults after tetralogy of Fallot repair. Am J Cardiol 2005;95:779-82.
13. Roman KS, Kellenberger CJ, Farooq S, MacGowan CK, Gilday DL, Yoo SJ. Comparative imaging of differential pulmonary blood flow in patients with congenital heart disease: Magnetic resonance imaging versus lung perfusion scintigraphy. Pediatr Radiol 2005;35:295-301.
14. Roman KS, Kellenberger CJ, Macgowan CK, et al. How is pulmonary arterial blood flow affected by pulmonary venous obstruction in children? A phase-contrast magnetic resonance study. Pediatr Radiol 2005;35:580-6.
15. Varaprasathan GA, Araoz PA, Higgins CB, Reddy GP. Quantification of flow dynamics in congenital heart disease: Applications of velocity-encoded cine MR imaging. Radiographics 2002;22:895-905; discussion 905-6.
16. Johnson TR, Goldmuntz E, McDonald-McGinn DM, Zackai EH, Fogel MA. Cardiac magnetic resonance imaging for accurate diagnosis of aortic arch anomalies in patients with 22q11.2 deletion. Am J Cardiol 2005;96:1726-30.
17. Grosse-Wortmann L, Al-Otay A, Goo HW, et al. Anatomical and functional evaluation of pulmonary veins in children by magnetic resonance imaging. J Am Coll Cardiol 2007;49:993-1002.
18. Babu-Narayan SV, Goktekin O, Moon JC, et al. Late gadolinium enhancement cardiovascular magnetic resonance of the systemic right ventricle in adults with previous atrial redirection surgery for transposition of the great arteries. Circulation 2005;111:2091-8.
19. Babu-Narayan SV, Kilner PJ, Li W, et al. Ventricular fibrosis suggested by cardiovascular magnetic resonance in adults with repaired tetralogy of fallot and its relationship to adverse markers of clinical outcome. Circulation 2006;113:405-13.
20. Barkhausen J, Ruehm SG, Goyen M, Buck T, Laub G, Debatin JF. MR evaluation of ventricular function: True fast imaging with steady-state precession versus fast low-angle shot cine MR imaging: Feasibility study. Radiology 2001;219:264-9.
21. Ichikawa Y, Sakuma H, Kitagawa K, et al. Evaluation of left ventricular volumes and ejection fraction using fast steady-state cine MR imaging: Comparison with left ventricular angiography. J Cardiovasc Magn Reson 2003;5:333-42.
22. Grothues F, Smith GC, Moon JC, et al. Comparison of interstudy reproducibility of cardiovascular magnetic resonance with two-dimensional echocardiography in normal subjects and in patients with heart failure or left ventricular hypertrophy. Am J Cardiol 2002;90:29-34.
23. Hudsmith LE, Petersen SE, Francis JM, Robson MD, Neubauer S. Normal human left and right ventricular and left atrial dimensions using steady state free precession magnetic resonance imaging. J Cardiovasc Magn Reson 2005;7:775-82.
24. Bloomer TN, Plein S, Radjenovic A, et al. Cine MRI using steady state free precession in the radial long axis orientation is a fast accurate method for obtaining volumetric data of the left ventricle. J Magn Reson Imaging 2001;14:685-92.
25. Hoffmann R, von Bardeleben S, ten Cate F, et al. Assessment of systolic left ventricular function: A multi-centre comparison of cineventriculography, cardiac magnetic resonance imaging, unenhanced and contrast-enhanced echocardiography. Eur Heart J 2005;26:607-16.
26. Bellenger NG, Davies LC, Francis JM, Coats AJ, Pennell DJ. Reduction in sample size for studies of remodeling in heart failure by the use of cardiovascular magnetic resonance. J Cardiovasc Magn Reson 2000;2:271-8.
27. Bellenger NG, Rajappan K, Rahman SL, et al. Effects of carvedilol on left ventricular remodelling in chronic stable heart failure: A cardiovascular magnetic resonance study. Heart 2004;90:760-4.
28. Strohm O, Schulz-Menger J, Pilz B, Osterziel KJ, Dietz R, Friedrich MG. Measurement of left ventricular dimensions and function in patients with dilated cardiomyopathy. J Magn Reson Imaging 2001;13:367-71.
29. Jenkins C, Bricknell K, Hanekom L, Marwick TH. Reproducibility and accuracy of echocardiographic measurements of left ventricular parameters using real-time three-dimensional echocardiography. J Am Coll Cardiol 2004;44:878-86.
30. Rosen BD, Gerber BL, Edvardsen T, et al. Late systolic onset of regional LV relaxation demonstrated in three-dimensional space by MRI tissue tagging. Am J Physiol Heart Circ Physiol 2004;287:H1740-6.

31. Castillo E, Osman NF, Rosen BD, et al. Quantitative assessment of regional myocardial function with MR-tagging in a multi-center study: Interobserver and intraobserver agreement of fast strain analysis with Harmonic Phase (HARP) MRI. J Cardiovasc Magn Reson 2005;7:783-91.
32. Petersen SE, Jung BA, Wiesmann F, et al. Myocardial tissue phase mapping with cine phase-contrast MR imaging: Regional wall motion analysis in healthy volunteers. Radiology 2006;238:816-26.
33. McGeoch RJ, Oldroyd KG. Pharmacological options for inducing maximal hyperaemia during studies of coronary physiology. Catheter Cardiovasc Interv 2008;71:198-204.
34. Schwitter J, Nanz D, Kneifel S, et al. Assessment of myocardial perfusion in coronary artery disease by magnetic resonance: A comparison with positron emission tomography and coronary angiography. Circulation 2001;103:2230-5.
35. Paetsch I, Jahnke C, Wahl A, et al. Comparison of dobutamine stress magnetic resonance, adenosine stress magnetic resonance, and adenosine stress magnetic resonance perfusion. Circulation 2004;110:835-42.
36. Al-Saadi N, Nagel E, Gross M, et al. Noninvasive detection of myocardial ischemia from perfusion reserve based on cardiovascular magnetic resonance. Circulation 2000;101:1379-83.
37. Giang TH, Nanz D, Coulden R, et al. Detection of coronary artery disease by magnetic resonance myocardial perfusion imaging with various contrast medium doses: First European multi-centre experience. Eur Heart J 2004;25:1657-65.
38. Rieber J, Huber A, Erhard I, et al. Cardiac magnetic resonance perfusion imaging for the functional assessment of coronary artery disease: A comparison with coronary angiography and fractional flow reserve. Eur Heart J 2006;27:1465-71.
39. Ingkanisorn WP, Kwong RY, Bohme NS, et al. Prognosis of negative adenosine stress magnetic resonance in patients presenting to an emergency department with chest pain. J Am Coll Cardiol 2006;47:1427-32.
40. Jahnke C, Nagel E, Gebker R, et al. Prognostic value of cardiac magnetic resonance stress tests: Adenosine stress perfusion and dobutamine stress wall motion imaging. Circulation 2007;115:1769-76.
41. Wahl A, Paetsch I, Gollesch A, et al. Safety and feasibility of high-dose dobutamine-atropine stress cardiovascular magnetic resonance for diagnosis of myocardial ischaemia: Experience in 1000 consecutive cases. Eur Heart J 2004;25:1230-36.
42. Kuijpers D, Janssen CH, van Dijkman PR, Oudkerk M. Dobutamine stress MRI. Part I. Safety and feasibility of dobutamine cardiovascular magnetic resonance in patients suspected of myocardial ischemia. Eur Radiol 2004;14:1823-8.
43. Kuijpers D, van Dijkman PR, Janssen CH, Vliegenthart R, Zijlstra F, Oudkerk M. Dobutamine stress MRI. Part II. Risk stratification with dobutamine cardiovascular magnetic resonance in patients suspected of myocardial ischemia. Eur Radiol 2004;14:2046-52.
44. Kaandorp TA, Lamb HJ, Bax JJ, van der Wall EE, de Roos A. Magnetic resonance imaging of coronary arteries, the ischemic cascade, and myocardial infarction. Am Heart J 2005;149:200-8.
45. Nagel E, Lehmkuhl HB, Bocksch W, et al. Noninvasive diagnosis of ischemia-induced wall motion abnormalities with the use of high-dose dobutamine stress MRI: Comparison with dobutamine stress echocardiography. Circulation 1999;99:763-70.
46. Hundley WG, Hamilton CA, Thomas MS, et al. Utility of fast cine magnetic resonance imaging and display for the detection of myocardial ischemia in patients not well suited for second harmonic stress echocardiography. Circulation 1999;100:1697-702.
47. Paetsch I, Jahnke C, Ferrari VA, et al. Determination of interobserver variability for identifying inducible left ventricular wall motion abnormalities during dobutamine stress magnetic resonance imaging. Eur Heart J 2006;27:1459-64.
48. Wacker CM, Hartlep AW, Pfleger S, Schad LR, Ertl G, Bauer WR. Susceptibility-sensitive magnetic resonance imaging detects human myocardium supplied by a stenotic coronary artery without a contrast agent. J Am Coll Cardiol 2003;41:834-40.
49. Friedrich MG, Niendorf T, Schulz-Menger J, Gross CM, Dietz R. Blood oxygen level-dependent magnetic resonance imaging in patients with stress-induced angina. Circulation 2003;108:2219-23.
50. Dharmakumar R, Arumana JM, Tang R, Harris K, Zhang Z, Li D. Assessment of regional myocardial oxygenation changes in the presence of coronary artery stenosis with balanced SSFP imaging at 3.0 T: Theory and experimental evaluation in canines. J Magn Reson Imaging 2008;27:1037-45.
51. Fieno DS, Shea SM, Li Y, Harris KR, Finn JP, Li D. Myocardial perfusion imaging based on the blood oxygen level-dependent effect using T2-prepared steady-state free-precession magnetic resonance imaging. Circulation 2004;110:1284-90.
52. Afridi I, Grayburn PA, Panza JA, Oh JK, Zoghbi WA, Marwick TH. Myocardial viability during dobutamine echocardiography predicts survival in patients with coronary artery disease and severe left ventricular systolic dysfunction. J Am Coll Cardiol 1998;32:921-6.
53. Allman KC, Shaw LJ, Hachamovitch R, Udelson JE. Myocardial viability testing and impact of revascularization on prognosis in patients with coronary artery disease and left ventricular dysfunction: A meta-analysis. J Am Coll Cardiol 2002;39:1151-8.
54. Wellnhofer E, Olariu A, Klein C, et al. Magnetic resonance low-dose dobutamine test is superior to SCAR quantification for the prediction of functional recovery. Circulation 2004;109:2172-4.
55. Baer FM, Theissen P, Schneider CA, et al. Dobutamine magnetic resonance imaging predicts contractile recovery of chronically dysfunctional myocardium after successful revascularization. J Am Coll Cardiol 1998;31:1040-8.
56. Sansoy V, Glover DK, Watson DD, et al. Comparison of thallium-201 resting redistribution with technetium-99m-sestamibi uptake and functional response to dobutamine for assessment of myocardial viability. Circulation 1995;92:994-1004.
57. Simonetti OP, Kim RJ, Fieno DS, et al. An improved MR imaging technique for the visualization of myocardial infarction. Radiology 2001;218:215-23.
58. Kim RJ, Fieno DS, Parrish TB, et al. Relationship of MRI delayed contrast enhancement to irreversible injury, infarct age, and contractile function. Circulation 1999;100:1992-2002.
59. Wagner A, Mahrholdt H, Holly TA, et al. Contrast-enhanced MRI and routine single photon emission computed tomography (SPECT) perfusion imaging for detection of subendocardial myocardial infarcts: An imaging study. Lancet 2003;361:374-9.
60. Rehwald WG, Fieno DS, Chen EL, Kim RJ, Judd RM. Myocardial magnetic resonance imaging contrast agent concentrations after reversible and irreversible ischemic injury. Circulation 2002;105:224-9.
61. Mahrholdt H, Wagner A, Holly TA, et al. Reproducibility of chronic infarct size measurement by contrast-enhanced magnetic resonance imaging. Circulation 2002;106:2322-7.
62. Mahrholdt H, Wagner A, Judd RM, Sechtem U. Assessment of myocardial viability by cardiovascular magnetic resonance imaging. Eur Heart J 2002;23:602-19.
63. Ricciardi MJ, Wu E, Davidson CJ, et al. Visualization of discrete microinfarction after percutaneous coronary intervention associated with mild creatine kinase-MB elevation. Circulation 2001;103:2780-3.
64. Lee VS, Resnick D, Tiu SS, et al. MR imaging evaluation of myocardial viability in the setting of equivocal SPECT results with (99m)Tc sestamibi. Radiology 2004;230:191-7.
65. Kitagawa K, Sakuma H, Hirano T, Okamoto S, Makino K, Takeda K. Acute myocardial infarction: Myocardial viability assessment in patients early thereafter comparison of contrast-enhanced MR imaging with resting (201)Tl SPECT. Single photon emission computed tomography. Radiology 2003;226:138-44.
66. Klein C, Nekolla SG, Bengel FM, et al. Assessment of myocardial viability with contrast-enhanced magnetic resonance imaging: Comparison with positron emission tomography. Circulation 2002;105:162-7.
67. Kuhl HP, Beek AM, van der Weerdt AP, et al. Myocardial viability in chronic ischemic heart disease: Comparison of contrast-enhanced magnetic resonance imaging with (18)F-fluorodeoxyglucose positron emission tomography. J Am Coll Cardiol 2003;41:1341-8.
68. Choi KM, Kim RJ, Gubernikoff G, Vargas JD, Parker M, Judd RM. Transmural extent of acute myocardial infarction predicts long-term improvement in contractile function. Circulation 2001;104:1101-7.
69. Beek AM, Kuhl HP, Bondarenko O, et al. Delayed contrast-enhanced magnetic resonance imaging for the prediction of regional functional improvement after acute myocardial infarction. J Am Coll Cardiol 2003;42:895-901.
70. Kim RJ, Wu E, Rafael A, et al. The use of contrast-enhanced magnetic resonance imaging to identify reversible myocardial dysfunction. N Engl J Med 2000;343:1445-53.

71. Schvartzman PR, Srichai MB, Grimm RA, et al. Nonstress delayed-enhancement magnetic resonance imaging of the myocardium predicts improvement of function after revascularization for chronic ischemic heart disease with left ventricular dysfunction. Am Heart J 2003;146:535-41.
72. Bello D, Shah DJ, Farah GM, et al. Gadolinium cardiovascular magnetic resonance predicts reversible myocardial dysfunction and remodeling in patients with heart failure undergoing beta-blocker therapy. Circulation 2003;108:1945-53.
73. Underwood SR, Bax JJ, vom Dahl J, et al. Imaging techniques for the assessment of myocardial hibernation. Report of a Study Group of the European Society of Cardiology. Eur Heart J 2004;25:815-36.
74. Schmidt A, Azevedo CF, Cheng A, et al. Infarct tissue heterogeneity by magnetic resonance imaging identifies enhanced cardiac arrhythmia susceptibility in patients with left ventricular dysfunction. Circulation 2007;115:2006-14.
75. Yan AT, Shayne AJ, Brown KA, et al. Characterization of the peri-infarct zone by contrast-enhanced cardiac magnetic resonance imaging is a powerful predictor of post-myocardial infarction mortality. Circulation 2006;114:32-9.
76. Wu KC, Zerhouni EA, Judd RM, et al. Prognostic significance of microvascular obstruction by magnetic resonance imaging in patients with acute myocardial infarction. Circulation 1998;97:765-72.
77. Abdel-Aty H, Zagrosek A, Schulz-Menger J, et al. Delayed enhancement and T2-weighted cardiovascular magnetic resonance imaging differentiate acute from chronic myocardial infarction. Circulation 2004;109:2411-6.
78. Abdel-Aty H, Cocker M, Tyberg JV, Friedrich MG. T2-weighted cardiovascular magnetic resonance detects acute myocardial ischemia before the onset of irreversible myocardial injury. Circulation 2007;116:772. (Abst)
79. Aletras AH, Tilak GS, Natanzon A, et al. Retrospective determination of the area at risk for reperfused acute myocardial infarction with T2-weighted cardiac magnetic resonance imaging: Histopathological and displacement encoding with stimulated echoes (DENSE) functional validations. Circulation 2006;113:1865-70.
80. Friedrich MG, Abdel-Aty H, Taylor A, Schulz-Menger J, Messroghli D, Dietz R. The salvaged area at risk in reperfused acute myocardial infarction as visualized by cardiovascular magnetic resonance. J Am Coll Cardiol 2008;51:1581-7.
81. Ibanez B, Prat-Gonzalez S, Speidl WS, et al. Early metoprolol administration before coronary reperfusion results in increased myocardial salvage: Analysis of ischemic myocardium at risk using cardiac magnetic resonance. Circulation 2007;115:2909-16.
82. Bragadeesh T, Jayaweera AR, Pascotto M, et al. Post-ischaemic myocardial dysfunction (stunning) results from myofibrillar oedema. Heart 2008;94:166-71.
83. Westenberg JJ, Lamb HJ, van der Geest RJ, et al. Assessment of left ventricular dyssynchrony in patients with conduction delay and idiopathic dilated cardiomyopathy: Head-to-head comparison between tissue Doppler imaging and velocity-encoded magnetic resonance imaging. J Am Coll Cardiol 2006;47:2042-8.
84. Russel IK, Zwanenburg JJ, Germans T, et al. Mechanical dyssynchrony or myocardial shortening as MRI predictor of response to biventricular pacing? J Magn Reson Imaging 2007;26:1452-60.
85. Chalil S, Stegemann B, Muhyaldeen S, et al. Intraventricular dyssynchrony predicts mortality and morbidity after cardiac resynchronization therapy: A study using cardiovascular magnetic resonance tissue synchronization imaging. J Am Coll Cardiol 2007;50:243-52.
86. Ypenburg C, Roes SD, Bleeker GB, et al. Effect of total scar burden on contrast-enhanced magnetic resonance imaging on response to cardiac resynchronization therapy. Am J Cardiol 2007;99:657-60.
87. White JA, Yee R, Yuan X, et al. Delayed enhancement magnetic resonance imaging predicts response to cardiac resynchronization therapy in patients with intraventricular dyssynchrony. J Am Coll Cardiol 2006;48:1953-60.
88. Chalil S, Foley PW, Muyhaldeen SA, et al. Late gadolinium enhancement-cardiovascular magnetic resonance as a predictor of response to cardiac resynchronization therapy in patients with ischaemic cardiomyopathy. Europace 2007;9:1031-7.
89. Chai P, Mohiaddin R. How we perform cardiovascular magnetic resonance flow assessment using phase-contrast velocity mapping. J Cardiovasc Magn Reson 2005;7:705-16.
90. Gatehouse PD, Keegan J, Crowe LA, et al. Applications of phase-contrast flow and velocity imaging in cardiovascular MRI. Eur Radiol 2005;15:2172-84.
91. Ku JP, Elkins CJ, Taylor CA. Comparison of CFD and MRI flow and velocities in an in vitro large artery bypass graft model. Ann Biomed Eng 2005;33:257-69.
92. Lotz J, Doker R, Noeske R, et al. In vitro validation of phase-contrast flow measurements at 3 T in comparison to 1.5 T: Precision, accuracy, and signal-to-noise ratios. J Magn Reson Imaging 2005;21:604-10.
93. Caruthers SD, Lin SJ, Brown P, et al. Practical value of cardiac magnetic resonance imaging for clinical quantification of aortic valve stenosis: Comparison with echocardiography. Circulation 2003;108:2236-43.
94. Sondergaard L, Lindvig K, Hildebrandt P, et al. Quantification of aortic regurgitation by magnetic resonance velocity mapping. Am Heart J 1993;125:1081-90.
95. Hundley WG, Li HF, Willard JE, et al. Magnetic resonance imaging assessment of the severity of mitral regurgitation. Comparison with invasive techniques. Circulation 1995;92:1151-8.
96. Friedrich MG, Schulz-Menger J, Poetsch T, Pilz B, Uhlich F, Dietz R. Quantification of valvular aortic stenosis by magnetic resonance imaging. Am Heart J 2002;144:329-34.
97. Kupfahl C, Honold M, Meinhardt G, et al. Evaluation of aortic stenosis by cardiovascular magnetic resonance imaging: Comparison with established routine clinical techniques. Heart 2004;90:893-901.
98. Dulce MC, Mostbeck GH, O'Sullivan M, Cheitlin M, Caputo GR, Higgins CB. Severity of aortic regurgitation: Interstudy reproducibility of measurements with velocity-encoded cine MR imaging. Radiology 1992;185:235-40.
99. Lin SJ, Brown PA, Watkins MP, et al. Quantification of stenotic mitral valve area with magnetic resonance imaging and comparison with Doppler ultrasound. J Am Coll Cardiol 2004;44:133-7.
100. Rebergen SA, Chin JG, Ottenkamp J, van der Wall EE, de Roos A. Pulmonary regurgitation in the late postoperative follow-up of tetralogy of Fallot. Volumetric quantitation by nuclear magnetic resonance velocity mapping. Circulation 1993;88:2257-66.
101. Schulz-Menger J, Abdel-Aty H, Busjahn A, et al. Left ventricular outflow tract planimetry by cardiovascular magnetic resonance differentiates obstructive from non-obstructive hypertrophic cardiomyopathy. J Cardiovasc Magn Reson 2006;8:741-6.
102. Schulz-Menger J, Strohm O, Waigand J, Uhlich F, Dietz R, Friedrich MG. The value of magnetic resonance imaging of the left ventricular outflow tract in patients with hypertrophic obstructive cardiomyopathy after septal artery embolization. Circulation 2000;101:1764-6.
103. Wilson JM, Villareal RP, Hariharan R, Massumi A, Muthupillai R, Flamm SD. Magnetic resonance imaging of myocardial fibrosis in hypertrophic cardiomyopathy. Tex Heart Inst J 2002;29:176-80.
104. Choudhury L, Mahrholdt H, Wagner A, et al. Myocardial scarring in asymptomatic or mildly symptomatic patients with hypertrophic cardiomyopathy. J Am Coll Cardiol 2002;40:2156-64.
105. Moon JC, Reed E, Sheppard MN, et al. The histologic basis of late gadolinium enhancement cardiovascular magnetic resonance in hypertrophic cardiomyopathy. J Am Coll Cardiol 2004;43:2260-4.
106. Adabag AS, Maron BJ, Appelbaum E, et al. Occurrence and frequency of arrhythmias in hypertrophic cardiomyopathy in relation to delayed enhancement on cardiovascular magnetic resonance. J Am Coll Cardiol 2008;51:1369-74.
107. McCrohon JA, Moon JC, Prasad SK, et al. Differentiation of heart failure related to dilated cardiomyopathy and coronary artery disease using gadolinium-enhanced cardiovascular magnetic resonance. Circulation 2003;108:54-9.
108. Assomull RG, Prasad SK, Lyne J, et al. Cardiovascular magnetic resonance, fibrosis, and prognosis in dilated cardiomyopathy. J Am Coll Cardiol 2006;48:1977-85.
109. Nazarian S, Bluemke DA, Lardo AC, et al. Magnetic resonance assessment of the substrate for inducible ventricular tachycardia in nonischemic cardiomyopathy. Circulation 2005;112:2821-5.
110. D'Ambrosio A, Patti G, Manzoli A, et al. The fate of acute myocarditis between spontaneous improvement and evolution to dilated cardiomyopathy: A review. Heart 2001;85:499-504.
111. Wallace KB. Doxorubicin-induced cardiac mitochondrionopathy. Pharmacol Toxicol 2003;93:105-15.

112. Piano MR. Alcoholic cardiomyopathy: Incidence, clinical characteristics, and pathophysiology. Chest 2002;121:1638-50.
113. Mobini R, Maschke H, Waagstein F. New insights into the pathogenesis of dilated cardiomyopathy: Possible underlying autoimmune mechanisms and therapy. Autoimmun Rev 2004;3:277-84.
114. Perel RD, Slaughter RE, Strugnell WE. Subendocardial late gadolinium enhancement in two patients with anthracycline cardiotoxicity following treatment for Ewing's sarcoma. J Cardiovasc Magn Reson 2006;8:789-91.
115. Wassmuth R, Lentzsch S, Erdbruegger U, et al. Subclinical cardiotoxic effects of anthracyclines as assessed by magnetic resonance imaging – a pilot study. Am Heart J 2001;141:1007-13.
116. Friedrich MG, Strohm O, Schulz-Menger J, Marciniak H, Luft FC, Dietz R. Contrast media-enhanced magnetic resonance imaging visualizes myocardial changes in the course of viral myocarditis. Circulation 1998;97:1802-9.
117. Abdel-Aty H, Boye P, Zagrosek A, et al. Diagnostic performance of cardiovascular magnetic resonance in patients with suspected acute myocarditis: Comparison of different approaches. J Am Coll Cardiol 2005;45:1815-22.
118. Gutberlet M, Spors B, Thoma T, et al. Suspected chronic myocarditis at cardiac MR: Diagnostic accuracy and association with immunohistologically detected inflammation and viral persistence. Radiology 2008;246:401-9.
119. Mahrholdt H, Goedecke C, Wagner A, et al. Cardiovascular magnetic resonance assessment of human myocarditis: A comparison to histology and molecular pathology. Circulation 2004;109:1250-8.
120. Mahrholdt H, Wagner A, Deluigi CC, et al. Presentation, patterns of myocardial damage, and clinical course of viral myocarditis. Circulation 2006;114:1581-90.
121. Wagner A, Schulz-Menger J, Dietz R, Friedrich MG. Long-term follow-up of patients paragraph sign with acute myocarditis by magnetic paragraph sign resonance imaging. MAGMA 2003;16:17-20.
122. Friedrich MG, Sechtem U, Schulz-Menger J, et al. Cardiovascular magnetic resonance in myocarditis: A JACC White Paper. J Am Coll Cardiol 2009;53:1475-87.
123. Skouri HN, Dec GW, Friedrich MG, Cooper LT. Noninvasive imaging in myocarditis. J Am Coll Cardiol 2006;48:2085-93.
124. Maceira AM, Joshi J, Prasad SK, et al. Cardiovascular magnetic resonance in cardiac amyloidosis. Circulation 2005;111:186-93.
125. Cheng AS, Banning AP, Mitchell AR, Neubauer S, Selvanayagam JB. Cardiac changes in systemic amyloidosis: Visualisation by magnetic resonance imaging. Int J Cardiol 2006;113:E21-3.
126. Schulz-Menger J, Wassmuth R, Abdel-Aty H, et al. Patterns of myocardial inflammation and scarring in sarcoidosis as assessed by cardiovascular magnetic resonance. Heart 2006;92:399-400.
127. Smedema JP, Snoep G, van Kroonenburgh MP, et al. Evaluation of the accuracy of gadolinium-enhanced cardiovascular magnetic resonance in the diagnosis of cardiac sarcoidosis. J Am Coll Cardiol 2005;45:1683-90.
128. Serra JJ, Monte GU, Mello ES, et al. Images in cardiovascular medicine. Cardiac sarcoidosis evaluated by delayed-enhanced magnetic resonance imaging. Circulation 2003;107:e188-9.
129. Moon JC, Sheppard M, Reed E, Lee P, Elliott PM, Pennell DJ. The histological basis of late gadolinium enhancement cardiovascular magnetic resonance in a patient with Anderson-Fabry disease. J Cardiovasc Magn Reson 2006;8:479-82.
130. Moon JC, Sachdev B, Elkington AG, et al. Gadolinium enhanced cardiovascular magnetic resonance in Anderson-Fabry disease. Evidence for a disease specific abnormality of the myocardial interstitium. Eur Heart J 2003;24:2151-5.
131. Anderson LJ, Holden S, Davis B, et al. Cardiovascular T2-star (T2*) magnetic resonance for the early diagnosis of myocardial iron overload. Eur Heart J 2001;22:2171-9.
132. Pennell DJ, Berdoukas V, Karagiorga M, et al. Randomized controlled trial of deferiprone or deferoxamine in beta-thalassemia major patients with asymptomatic myocardial siderosis. Blood 2006;107:3738-44.
133. Anderson LJ, Wonke B, Prescott E, Holden S, Walker JM, Pennell DJ. Comparison of effects of oral deferiprone and subcutaneous desferrioxamine on myocardial iron concentrations and ventricular function in beta-thalassaemia. Lancet 2002;360:516-20.
134. Petersen SE, Selvanayagam JB, Wiesmann F, et al. Left ventricular non-compaction: Insights from cardiovascular magnetic resonance imaging. J Am Coll Cardiol 2005;46:101-5.
135. Korcyk D, Edwards CC, Armstrong G, et al. Contrast-enhanced cardiac magnetic resonance in a patient with familial isolated ventricular non-compaction. J Cardiovasc Magn Reson 2004;6:569-76.
136. Deetjen AG, Conradi G, Mollmann S, Rad A, Hamm CW, Dill T. Value of gadolinium-enhanced magnetic resonance imaging in patients with Tako-Tsubo-like left ventricular dysfunction. J Cardiovasc Magn Reson 2006;8:367-72.
137. Fischer R, Schirdewan A, Kumar A, Gapelyuk A, Schulz-Menger J, Dietz R. Cardiac magnetic resonance and cardiac magnetic field mapping in a patient with stress-induced cardiomyopathy (tako-tsubo). Pacing Clin Electrophysiol 2006;29:1442-4.
138. Haghi D, Fluechter S, Suselbeck T, Borggrefe M, Papavassiliu T. Delayed hyperenhancement in a case of Takotsubo cardiomyopathy. J Cardiovasc Magn Reson 2005;7:845-7.
139. Nienaber CA, von Kodolitsch Y, Nicolas V, et al. The diagnosis of thoracic aortic dissection by noninvasive imaging procedures. N Engl J Med 1993;328:1-9.
140. Hoffmann U, Globits S, Schima W, et al. Usefulness of magnetic resonance imaging of cardiac and paracardiac masses. Am J Cardiol 2003;92:890-5.
141. Kefer J, Coche E, Legros G, et al. Head-to-head comparison of three-dimensional navigator-gated magnetic resonance imaging and 16-slice computed tomography to detect coronary artery stenosis in patients. J Am Coll Cardiol 2005;46:92-100.
142. Kim WY, Danias PG, Stuber M, et al. Coronary magnetic resonance angiography for the detection of coronary stenoses. N Engl J Med 2001;345:1863-9.